

Model based OPC for implant layer patterning considering wafer topography proximity (W3D) effects

Songyi Park, Hyungjoo Youn, Noyoung Chung, Jaeyeol Maeng, Sukjoo Lee and Jahum Ku
Samsung Electronics, Nongseo-Dong, Giheung-Gu, Yongin-City, Gyeonggi-Do, 446-711, Korea

*Xiaobo Xie, *Song Lan, *Mu Feng, *Venu Vellanki, *Joobyoung Kim, *Stanislas Baron, and *Hua-yu Liu

*Brion Technologies, Inc., an ASML company, 4211 Burton Drive, Santa Clara, CA 95054, USA

**Stefan Hunsche, **Soung-Su Woo, **Seung-Hoon Park, and **Jong-Tai Yoon
**ASML Korea Co., Ltd. (Republic of Korea)

ABSTRACT

Implant layer patterning is becoming challenging with node shrink due to decreasing critical dimension (CD) and usage of non-uniform reflective substrates without bottom anti-reflection coating (BARC).

Conventional OPC models are calibrated on a uniform silicon substrate and the model does not consider any wafer topography proximity effects from sub-layers. So the existing planar OPC model cannot predict the sub-layer effects such as reflection and scattering of light from substrate and non-uniform interfaces. This is insufficient for layers without BARC, e.g., implant layer, as technology node shrinks.

For 45-nm and larger nodes, the wafer topography proximity effects in implant layer have been ignored or compensated using rule based OPC. When the node reached 40 nm and below, the sub-layer effects cause undesired CD variation and resist profile change. Hence, it is necessary to model the wafer topography proximity effects accurately and compensate them by model based OPC. Rigorous models can calculate the wafer topography proximity effects quite accurately if well calibrated. However, the run time for model calibration and OPC compensation are long by rigorous models and they are not suitable for full chip applications. In this paper, we demonstrate an accurate and rapid method that considers wafer topography proximity effects using a kernel based model. We also demonstrate application of this model for full chip OPC on implant layers.

Keywords: implant layer model, computational lithography, OPC, optical proximity correction, wafer topography, kernel.

1. INTRODUCTION

In projection photolithography, photoresist is exposed to light patterns that are formed by a photomask and an optical projection system. The light intensity distribution in the photoresist induces chemical reactions and thus mainly determines the solubility of the photoresist during development. This greatly affects the final pattern transfer onto the wafer substrate. In critical layer patterning, a bottom anti-reflection coating (BARC) layer is always used underneath the photoresist to minimize the back reflection from the substrate. Hence, the influence of the wafer topographic structure on the light intensity distribution in the photoresist is mitigated and the substrate can be considered as uniform in lithographic modeling. However, in non-critical layers such as implant layer patterning, the BARC is not desired due to cost and yield concerns along with the technical difficulty of clearing the BARC layer afterwards. The wafer structure of pre-gate implant layer has active silicon (RX) and silicon oxide shallow trench isolation (STI) patterns. Both materials can cause light reflection and scattering back to the photoresist layer and alter the aerial image formed by the photomask patterns. Figure 1 shows an illustration of the wafer topography proximity (W3D) effects for simple situation of normal incident light. The multiple reflections between the top and bottom interfaces of the photoresist layer form standing wave. The RX and STI regions have different reflection coefficients due to different material indices of refraction and

layer structures and therefore they can have quite different standing wave light distributions. At the boundary of the RX and STI regions, light interference can occur, as shown in Figure 2. In real processing situations, the side wall angle

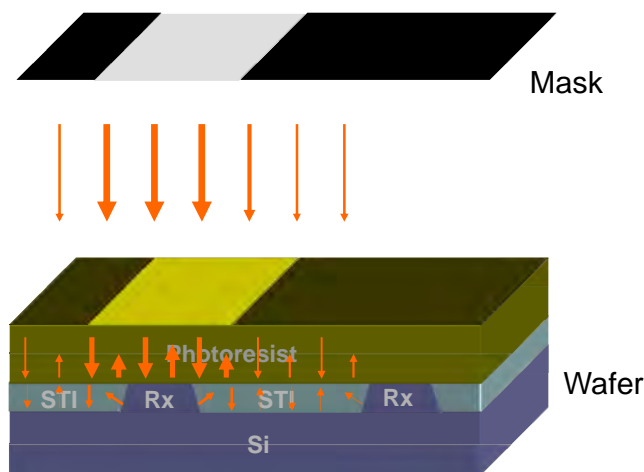


Figure 1. Illustration of implant layer wafer topography proximity (W3D) effects for normal incident light.

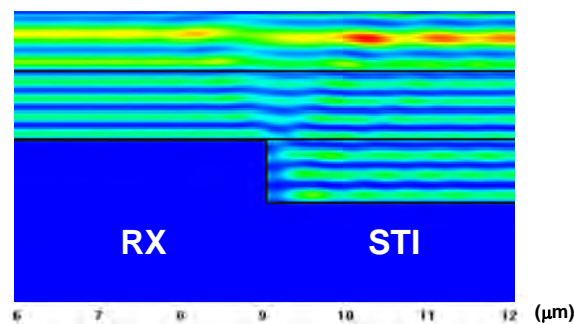


Figure 2. Rigorously calculated light intensity distribution around the boundary of the active silicon (RX) and silicon oxide shallow trench isolation (STI) regions.

(SWA) at the RX and STI boundary, which is the slope of the RX/STI interface, can deviate from vertical angle and the incident light is usually oblique rather than normal. The alteration of the light intensity distribution as compared to the case of uniform substrate can be severe. The W3D effects can reach as far as a distance on the order of micron away from the boundary and result in undesired critical dimension (CD) variations of tens of nanometers along with resist profile changes¹.

The implant layer patterns are usually much larger than those critical layer patterns and therefore they have loose CD error tolerance. Before the 45-nm node, the W3D effects can be neglected or can just be corrected by rule based optical proximity correction (OPC) to meet the requirement. However, as the technology node shrinks to 40 nm and below, the rule based OPC is not sufficient to compensate the undesired CD variations. Model based OPC becomes necessary.

Modeling of W3D effects is very complicated and time consuming. Rigorous calculations by finite-difference time-domain (FDTD)² or rigorous coupled wave analysis (RCWA) method can only simulate very small regions with reasonable CPU and memory resources. Although the simulated results are usually accurate if well calibrated with all the physical parameters, the run time is usually long. This makes it only feasible for detailed feature study but not for full chip OPC modeling.

Besides, the pre-patterned wafer can have process dependent feature variations across the wafer such as SWA³. The SWA between silicon and silicon oxide can change with line pitch size and the line CD is very sensitive to the SWA.

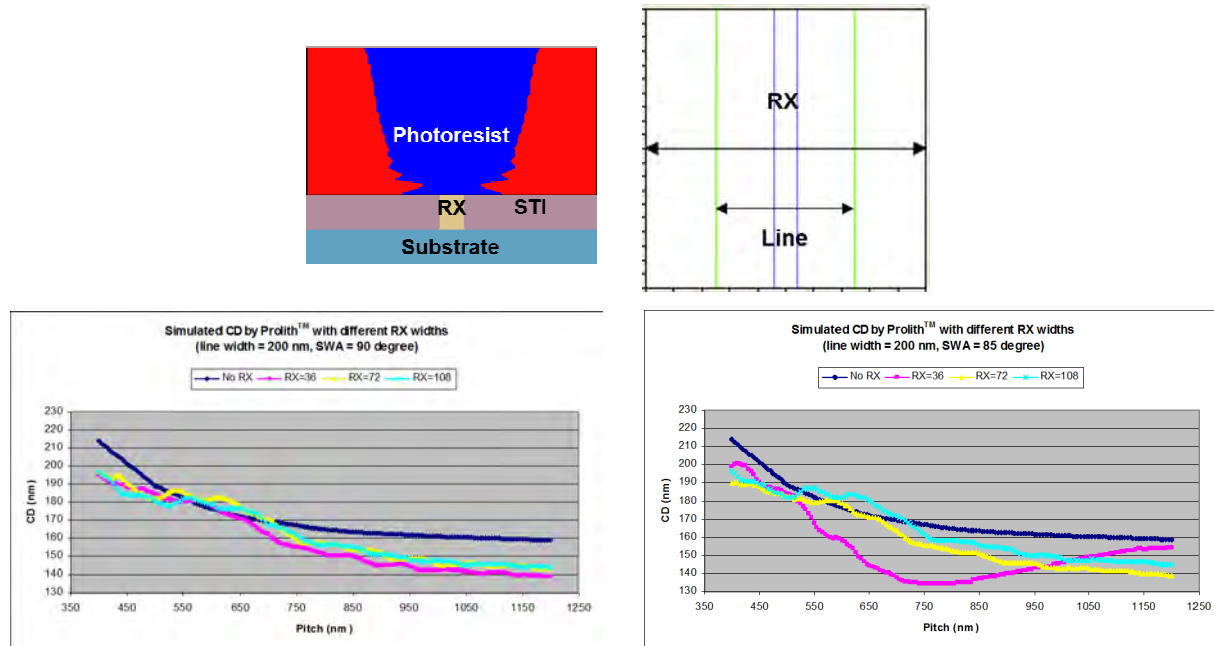


Figure 3. Prolith™ simulation of wafer topography proximity effects. The mask line width is fixed at 200 nm with different pitch sizes. The underlining RX line widths are 36 nm, 72 nm, and 108 nm. Two side wall angle (SWA) values of 90 and 85 degrees are used.

Figure 3 shows line CD simulation by rigorous simulator Prolith™ from KLA-Tencor. RCWA method is employed in the calculation. The mask is a dark field binary mask and it has regular line-space pattern with line width fixed at 200 nm. The wafer has an RX line located at the center of the mask line and its width is varied between 36 nm, 72 nm, and 108 nm. The rest of the wafer has STI. Two SWA settings of 90 degree and 85 degree are used and line CD versus pitch is plotted in Figure 3. As can be seen from the plots, the through pitch line CD for the uniform wafer (no RX) has smooth trend. For the wafer with RX line of different widths, the through pitch CD curves show wavy trends due to complicated light interference at different pitch conditions. Between two SWA settings, line CD values and curve trends change significantly. For example, for curves with RX width of 36 nm, the CD difference at 650-nm pitch is as large as 25 nm. As the SWA information is hard to obtain without taking experimental cross section measurement of the wafer, it becomes uncertain in production environment. This feature uncertainty even makes OPC compensation by rigorous models unreliable.

Model based OPC to compensate the W3D effects in the implant layer does not require the accuracy as that in the critical layers. But reasonable model calibration run time and fast OPC throughput are more desired. Sub-layer aware OPC has been studied in the literature^{4,5} but only limited test patterns were included and no full chip coverage was mentioned. Based on the Tachyon modeling framework, Brion has developed fast models for full chip applications. One model takes more physical approach and the preliminary results are given elsewhere⁶. In this paper we present a kernel based model, in which we modified the conventional Tachyon modeling flow to consider non-uniform wafer substrate and introduced specific kernel based filters to tackle the aerial image alteration and CD changes due to the W3D effects. The paper will show that the calibration using this Tachyon W3D model can yield model CD errors to be less than 10% for large scale full chip patterns. The model can also be used in the model based OPC for mask correction with fast throughput. The resulting mask has the wafer CDs within reasonable error range of the model predicted CDs.

2. TACHYON FAST W3D MODEL

Conventional OPC model only takes uniform wafer substrate. The mask image from GDS is taken to go through a modeled optical projection system. In the near field of the wafer, uniform film stack layers on the substrate are taken into account to obtain the aerial image in the photoresist. To accommodate the W3D effects, we take the approach of

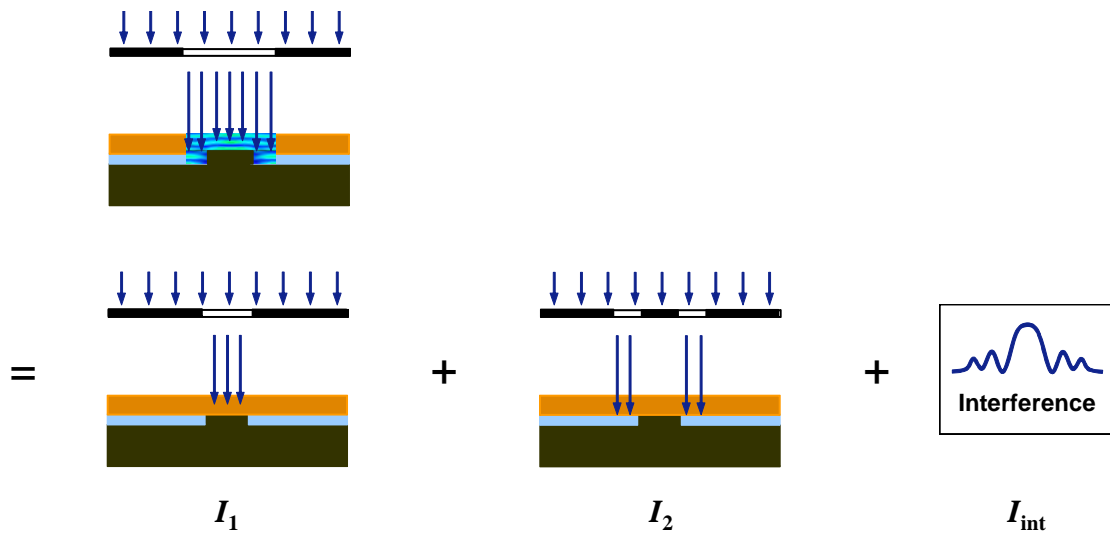


Figure 4. Tachyon model to consider W3D effects. The total effects can be separated into sub-effects in the model.

calculating aerial images in different regions with different wafer film stacks and then constructing the final aerial image out of sub-area aerial images with the help of the physical understanding of light interference and the empirical observation of wafer measurement data. This approach can be explained by Figure 4. The aerial image with W3D effects can be calculated by decomposing it into three parts, each of which can be taken by conventional Tachyon modeling or by additionally introducing modeling parameters and terms. In the regions where the underlining layer is a patch of RX layer or STI layer, the film stacks can be considered uniform in those regions. The aerial image in those regions can be calculated as usual by taking into account the wafer film stacks of RX or STI, respectively. The corresponding aerial images are I_1 and I_2 , respectively. In the vicinity of the RX/STI boundary, the W3D effects are severe. They are caused by the light interference between I_1 and I_2 as they overlap around the RX/STI interface. This interference term I_{int} can be modeled as kernel based filters. The filter kernels are designed based on the observation of wafer data. These filters are empirical filters that only affect the surroundings of the RX/STI boundary. Depending on the trend and severity of the W3D effects, different kinds of specially designed filters with adjustable parameters can be employed in the model calibration. So in a mathematical form, the final aerial image calculation can be expressed as follows.

$$\begin{aligned}
 I &= I_1 + I_2 + I_{\text{int}} \\
 &= I_1 + I_2 + \sum I_f(I_1, I_2, \text{kernel})
 \end{aligned}
 \tag{1}$$

In this Tachyon W3D modeling framework, the sub-layer information, which describes the layout of RX and STI regions, is taken as a virtual mask with an additional GDS for the model input. As illustrated in Figure 5, an intermediate aerial image can be calculated with the mask GDS, the sub-layer GDS, optical illumination configuration, and wafer film

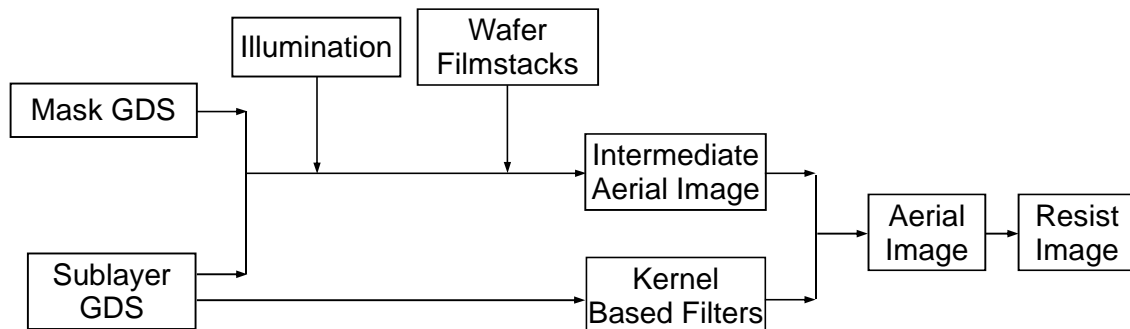


Figure 5. Tachyon framework of W3D modeling.

stacks of RX and STI. Additional kernel based filters are applied onto the intermediate aerial image to get the final aerial image. This final aerial image can be taken by a resist model to obtain a resist image as in a conventional Tachyon model.

This Tachyon W3D model can be considered as a lumped model for the W3D effects. It only takes limited physical parameters while leaving others to be handled by adjustable filters. Generally it does not have the accuracy provided by rigorous calculations. However, it offers quite a few advantages for an OPC model. Firstly, the mature uniform film stack modeling only needs to be modified to take the W3D effects. The conventional Tachyon modeling capability can be re-used. Secondly, the aerial image calculation is decomposed into several components. The first and second components I_1 and I_2 conform to the conventional Tachyon model and they can easily be calibrated with wafer data that are measured on a large RX or STI region. Some optical exposure conditions can be cross checked between these two regions to ensure model reliability. Thirdly, kernel based filters are based on empirical observations. They are flexible to fit different phenomena without taking all physical parameters. This is especially helpful if some physical parameters are difficult to obtain in production, e.g., SWA. They are also expandable to include newly observed trends if the filters used in the model are not sufficient.

3. RESULTS AND DISCUSSIONS

The Tachyon W3D modeling flow was used to calibrate several W3D models with varieties of line-space pitch patterns of both mask GDS and sub layer GDS and with both bright and dark field masks. Figure 6 shows some of the patterns used in the W3D model calibration. The first two patterns a and b are line-space pattern in STI and RX sub-layer regions. They can be handled by the conventional Tachyon model and were used to obtain non-W3D optical model parameters. The patterns c and d have RX sub-layer line in the mask line or/and mask space. BARC was not used in the wafer film stacks. The wafer data showed the influence of RX sub-layer line on CD values. In the pattern group where the RX line is within the mask line for a dark field mask, similar through pitch CD trend as the simulation result in Figure 3 was observed. The W3D effects were evaluated from the wafer CD data from patterns c and d, and kernel based W3D filters were tried and selected in the model calibration.

A summary of the result of one of the calibrated models is shown in Figure 7. Patterns a, c, and d were included in the calibration. The green curve is the CD error for different patterns with a model that was calibrated with W3D and the orange curve is from a conventional model. The conventional model only used aerial images in the RX and STI regions but did not include I_{int} component. It is clear that the W3D model outperforms the non-W3D model. For the W3D model, the CD error range is within 10%. The CD errors from the non-W3D model can reach to about 18%. Please note that the non-W3D model was calibrated against the wafer data so some W3D effects might be absorbed by resist terms. This comparison shows the effectiveness of the Tachyon W3D model in calibration.

The calibrated models were used to do OPC. Although the filters accounting for the W3D effects are long due to the fact that CD change can occur at quite far distances from the RX/STI boundary, the OPC run time is still reasonable. In a benchmark test, we compared the OPC run time of a conventional Tachyon model and a W3D Tachyon model with a full chip layout. The run time increase is merely 1.4 times, which is acceptable for production.

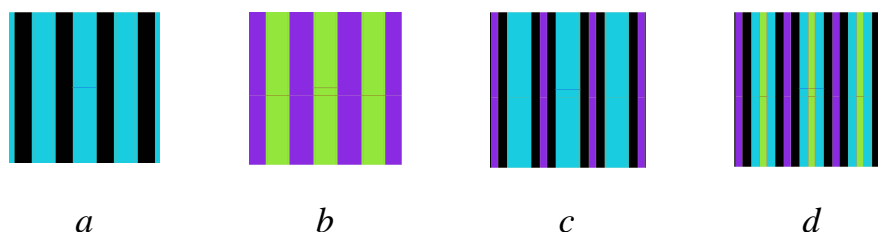


Figure 6. Some example W3D patterns used in the model calibration and verification. The black and purple colors correspond to STI and RX background. The cyan color is the mask line on STI and the light green color is the mask line on RX. a) line-space on STI; b) line-space on RX; c) line-space pattern with RX lines in either line or space; d) line-space pattern with RX line in both line and space.

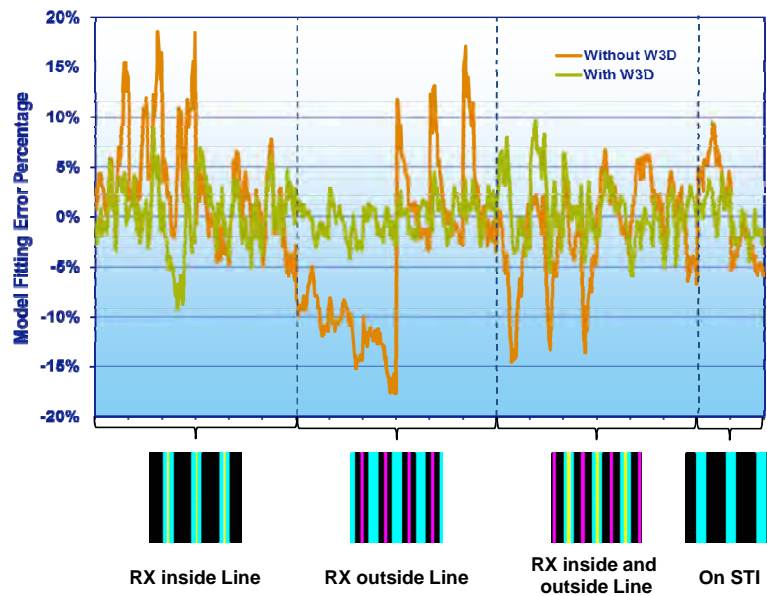


Figure 7. Shown above are the model calibration fit errors from two models: regular model without consideration of substrate non-uniformity and a model considering the wafer topography proximity (W3D) effects. W3D model can meet the $\pm 10\%$ error requirement.

The post-OPC masks include more patterns than those in calibration and were exposed with the same condition as the calibration mask. The wafer measurement data were used to verify the prediction capability of the W3D model. By comparing the wafer CD and the model predicted CD, the prediction errors were within 13%. Figure 8 shows a histogram of the error percentage distribution. Most of the patterns have small error percentage. Among all 432 CD measurements, only 14 CD values have errors larger than 10%.

The calibrated model was also used to check post-OPC SEM images to see if the model can catch the resist contour and predict the trend. Figure 9 shows one SEM image overlaid with the model predicted contour. It is a pattern of horizontal mask space crossing a vertical RX sub-layer space. The model predicted resist contour agrees well with the SEM image. This 2D pattern was not included in the calibration. However, the model still catches the wavy resist contour, especially at the center of the space where the mask space is straight as compared with the waist-like resist contour. The kernel based filters effectively take W3D effects into account.

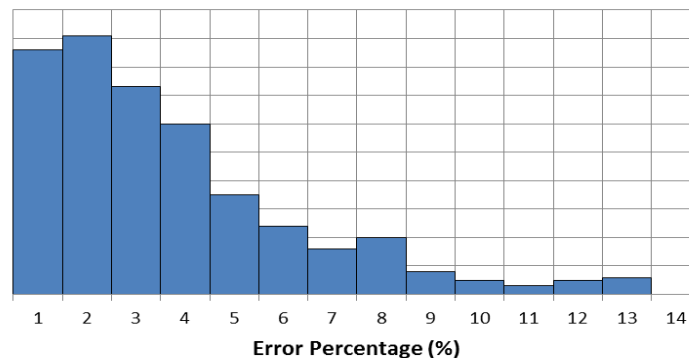


Figure 8. Histogram of the error percentage between model predicted CD and post-OPC wafer CD.

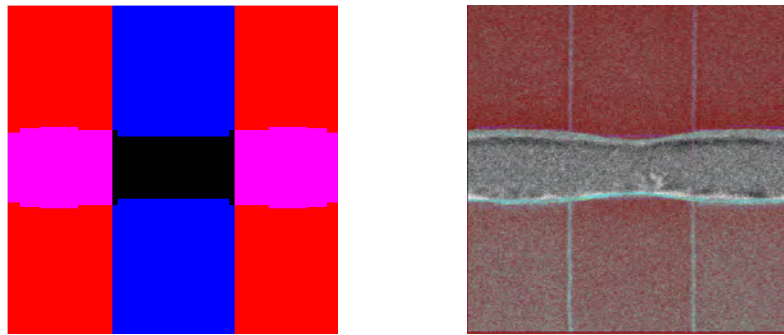


Figure 9. The W3D model predicted resist contour overlaid with post-OPC SEM image. The pattern is a horizontal mask space crossing a vertical RX sub-layer space as shown in the left plot. The blue, red, and pink colors correspond to mask line on STI, mask line on RX, and mask space on RX.

4. CONCLUSIONS AND SUMMARY

In summary, a kernel based W3D model on top of conventional Tachyon modeling framework was developed. Both model calibration and post-OPC model verification show promising results. This Tachyon W3D modeling can be improved by introducing more types of filters to account for more data trends that will be observed in the patterns not studied yet. Moreover, handling of multiple sub-layers can in principle be extended. This is very useful for post-gate implant layer where both RX and poly sub-layers are present.

REFERENCES

- [1] Bailey, T. C., McIntyre, G., Zhang, B., Deschner, R. P., Mehta, S., Song, W., Lee, H.-R., Hu, Y., and Brodsky, M. J., "Reflectivity-induced variation in implant layer lithography," Proc. SPIE 6924, 69244F (2008).
- [2] Erdmann, A., Kalus, C., Schmöller, T., Klyonova, Y., Sato, T., Endo, A., Shibata, T., and Kobayashi Y., "Rigorous simulation of exposure over non-planar wafers," Proc. SPIE 5040, 101-111 (2003).
- [3] Shao, D., Bailey, T. C., Stobert, I., Popova, I., and Chang, C. S., "Substrate aware OPC rules for edge effect in block levels," Proc. SPIE 7823, 78233U (2010).
- [4] Song, H., Shiely, J., Su, I., Zhang, L., and Lei, W.-K., "Wafer topography proximity effect modeling and correction for implant layer patterning," Proc. SPIE 7488, 74883F (2009).
- [5] Stock, H.-J., Bomholt, L., Krüger, D., Shiely, J., Song, H., and Voznesenskiy, N., "Virtual fab flow for wafer topography aware OPC," Proc. SPIE 7640, 67401U (2010).
- [6] Liu, P., Zhang, Z., Lan, S., Zhao, Q., Feng, M., Liu, H.-Y., Velanki, V., and Lu, Y.-W., "A full-chip 3D computational lithography framework," To be presented to SPIE Advanced Lithography 2012.